









Effects of high-energy proton irradiation on the superconducting properties of Fe(Se,Te) thin films

G Sylva^{1,2} , E Bellingeri¹, C Ferdeghini¹, A Martinelli¹ , I Pallecchi¹ ,
L Pellegrino¹ , M Putti^{1,2}, G Ghigo³, L Gozzelino³ , D Torsello³ ,
G Grimaldi⁴ , A Leo^{4,5}, A Nigro^{4,5} and V Braccini¹ 

¹ National Research Council CNR-SPIN Genova, C.so Perrone 24, I-16152 Genova, Italy

² Physics Department, University of Genova, via Dodecaneso 33, 16146 Genova, Italy

³ Department of Applied Science and Technology, Politecnico di Torino and INFN Sezione di Torino, C.so Duca degli Abruzzi 24, I-10129 Torino, Italy

⁴ National Research Council CNR-SPIN Salerno, Via Giovanni Paolo II 132, I-84084 Fisciano (SA), Italy

⁵ Physics Department 'E.R. Caianiello', University of Salerno, Via Giovanni Paolo II 132, I-84084 Fisciano (SA), Italy

E-mail: valeria.braccini@spin.cnr.it

Received 7 December 2017, revised 20 February 2018

Accepted for publication 2 March 2018

Published 28 March 2018



Abstract

In this paper we explore the effects of 3.5 MeV proton irradiation on Fe(Se,Te) thin films grown on CaF₂. In particular, we carry out an experimental investigation with different irradiation fluences up to $7.30 \cdot 10^{16} \text{ cm}^{-2}$ and different proton implantation depths, in order to clarify whether and to what extent the critical current is enhanced or suppressed, what are the effects of irradiation on the critical temperature, resistivity, and critical magnetic fields, and finally what is the role played by the substrate in this context. We find that the effect of irradiation on superconducting properties is generally small compared to the case of other iron-based superconductors. The irradiation effect is more evident on the critical current density J_c , while it is minor on the transition temperature T_c , normal state resistivity ρ , and on the upper critical field H_{c2} up to the highest fluences explored in this work. In more detail, our analysis shows that when protons implant in the substrate far from the superconducting film, the critical current can be enhanced up to 50% of the pristine value at 7 T and 12 K; meanwhile, there is no appreciable effect on critical temperature and critical fields together with a slight decrease in resistivity. On the contrary, when the implantation layer is closer to the film–substrate interface, both critical current and temperature show a decrease accompanied by an enhancement of the resistivity and lattice strain. This result evidences that possible modifications induced by irradiation in the substrate may affect the superconducting properties of the film via lattice strain. The robustness of the Fe(Se,Te) system to irradiation-induced damage makes it a promising compound for the fabrication of magnets in high-energy accelerators.

Keywords: iron-based superconductors, proton irradiation, thin films

(Some figures may appear in colour only in the online journal)

Introduction

Effects of irradiation on iron-based superconductors (FeSCs) have been investigated since their discovery with several

goals in mind, namely gaining information on fundamental properties such as gap symmetry and suppression of the critical temperature T_c by impurity scattering [1, 2], investigating vortex physics and flux pinning in view of applications in

magnet fabrication [3], and testing the robustness or deterioration of superconducting properties by irradiations for application in high-energy accelerators.

Given the unconventional pairing mechanism and symmetry of the order parameter in FeSCs, it was initially expected that irradiation damage would significantly suppress the superconducting properties. On the contrary, only mild T_c suppression and visible enhancement of the critical current density J_c were observed in the so-called 122 and 1111 FeSCs families (see [3] for a review). In particular, in the 1111 family, J_c values up to $2 \cdot 10^7 \text{ A cm}^{-2}$ were measured after heavy ion irradiation [4].

In the 11 family, different results have been reported depending on the phase, the type of particle, and its energy. For example, thin films grown on LaAlO_3 by our group and irradiated with neutrons duplicated their critical current at 15 K with no change in T_c [5]. Conversely, an increase of T_c was found after neutron [6], electron [7], and proton [8] irradiation. This remarkable result highlights a mechanism for an increase in transition temperature, which can over-compensate for the detrimental effect of disorder on T_c . Surprising results have been found specifically in FeSe [7] and Fe(Se,Te) [8] samples. In [7], a T_c enhancement of 0.4 K upon electron irradiation was detected in FeSe single crystals, and was interpreted by the authors as due to local strengthening of the magnetic pairing mechanism by irradiation-induced defects. In Fe(Se,Te) thin films irradiated by low-energy protons, not only was J_c ($T = 4.2 \text{ K}$, $H = 0$) increased by 55% and the pinning force increased in the high-field regime upon irradiation, but remarkably a simultaneous T_c enhancement by 0.5 K was detected [8]. The authors of [8] considered possible mechanisms for T_c enhancement in Fe(Se,Te) films, namely phonon-related interface effects [9], chemical effects related to excess Fe at interstitial sites, and Se/Te ratio [10] and strain effects [11]; and on the basis of structural analysis they interpreted their results in terms of the coexistence of nanoscale regions subject to compressive and tensile strain, originated by the irradiation defects. On the other hand, a more extended investigation carried out on heavy ion-irradiated $\text{FeSe}_{0.4}\text{Te}_{0.6}$ single crystals yielded results on superconducting properties that were not systematic and not reproducible [12]; this was despite a significant effect in terms of vortex-pinning enhancement on $\text{FeSe}_{0.45}\text{Te}_{0.55}$ crystals proven on the atomic scale [13]. Recently, on the contrary, Fe(Se,Te) thin films grown on CaF_2 were reported to show a decrease in T_c up to 7 K upon irradiation with 3.5 MeV protons [14].

Clearly, before conjecturing on the mechanisms for T_c and J_c enhancements, understanding irradiation effects in 11 FeSCs requires a larger systematic experimental investigation carried out with different fluences and energies, as well as a comprehensive comparison of samples available in the literature. The experimental results should be correlated with the expected disorder created in the sample by irradiation.

In this paper we aim to address several questions concerning the effects of 3.5 MeV proton irradiation of $\text{FeSe}_{0.5}\text{Te}_{0.5}$ films, namely whether and to what extent the critical current can be enhanced, what is the effect on the

strain, critical temperature, and critical magnetic fields, and finally what is the role played by the substrate. The latter is a crucial and complex issue, unavoidable in the case of thin films: besides defects created in the film, impinging protons produce modifications of the substrate that in turn have influence on the properties of the film. To address this issue, we compare results obtained in different experimental conditions, i.e. with the same defect density created by protons in the film but with different proton implantation depths into the substrate. This is obtained by lowering the proton energy with the interposition of a thin aluminium (Al) foil between the proton beam and the sample.

Experimental details

The thin films used for this irradiation experiment were deposited on oriented 001 CaF_2 single crystals in an ultra-high vacuum pulsed laser deposition (PLD) system equipped with a Nd:YAG laser at 1024 nm using a $\text{FeSe}_{0.5}\text{Te}_{0.5}$ target prepared by direct synthesis with a two-step method [15]. The deposition was carried out at a residual gas pressure of 10^{-8} mbar while the substrate was kept at 350 °C. The parameters of the laser used during the deposition were 3 Hz as the laser repetition rate, 2 J cm^{-2} as the laser fluency (2 mm² spot size), and 5 cm as the distance between the target and the sample; the parameters were optimised to obtain high-quality epitaxial Fe(Se,Te) thin films [16].

Five films 100 nm thick were prepared for irradiation. Three of them, indicated in the following as samples A, B, and C, were patterned and designated for transport measurements; meanwhile, samples D and E were analysed with x-ray diffraction. Before irradiation, all films were analysed with x-ray diffraction using a four-circle diffractometer. This analysis confirmed the phase purity of all films and the optimum epitaxial growth of all films. Φ scans revealed that films grow rotated by 45° with respect to the a axis due to good matching with half of the diagonal of the CaF_2 crystalline cell, as already reported [17].

By using the 00 l diffraction patterns, the values of the c cell parameter for the different samples were evaluated by means of Rietveld refinement with the programme Fullprof. The instrumental resolution function and the zero-shift parameters were refined using the CaF_2 substrate as reference; diffraction lines were modelled by a Thompson–Cox–Hastings pseudo-Voigt convoluted with an axial divergence asymmetry function. The obtained values were fixed, and, by imposing a full c -axis texturing, the parameters pertaining to the $\text{FeSe}_{0.5}\text{Te}_{0.5}$ thin films were refined, i.e. the lattice parameter c and the Lorentzian strain parameter. Lattice micro-strain along [00 l] was evaluated by the refined strain parameters, and the broadening of diffraction lines was analysed by means of the Williamson–Hall plot method [18]. Generally, in the case where size effects are negligible and the micro-strain is isotropic, a straight line passing through all the points in the plot and through the origin has to be observed, where the slope provides the micro-strain: the higher the slope, the higher the micro-strain. If the broadening is not

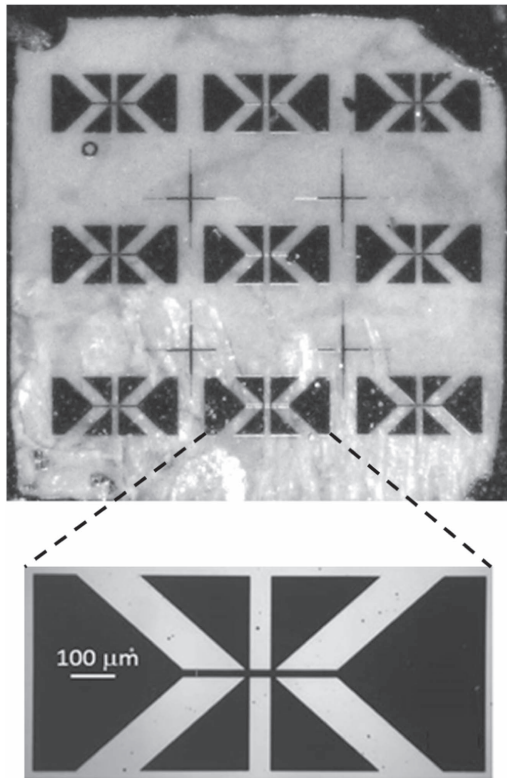


Figure 1. Optical viewgraph of a Fe(Se,Te) thin-film sample showing the nine Hall bar-shaped micro-bridges, and a magnification of a single 20 micron wide micro bridge with voltage pads 50 μm apart.

isotropic, size and strain effects along particular crystallographic directions can be obtained by considering different orders of the same reflection. In the present case, all the analysed diffraction lines pertain to the same 00 l family of planes.

In order to allow the measurement of critical current, the films designated for transport measurements were patterned through standard optical photolithography, and the etching was performed by water-cooled argon ion milling (argon ion energy 500 eV). After the milling process, the photoresist was removed by mild sonication in acetone for a few tens of seconds and dried in nitrogen air. Nine Hall bar-shaped micro-bridges $20 \times 50 \mu\text{m}^2$ in size were realised (see figure 1). Single Hall bars or groups of Hall bars were then selectively irradiated with different fluence values as detailed in the following.

The films were irradiated with 3.5 MeV protons at the CN Van de Graaf accelerator of the Istituto Nazionale di Fisica Nucleare—Laboratori Nazionali di Legnaro, Italy. The ion beam was parallel to the c -axis of the films, and the proton flux was always kept below $10^{12} \text{ cm}^{-2} \text{ s}^{-1}$ in order to minimise the heating of the samples under irradiation. In order to investigate the influence of the proton's implantation depth on the structural and electrical properties of the films, some of the samples were directly irradiated with 3.5 MeV protons while others were irradiated with protons decelerated through the interposition of an 80 μm thick Al foil. This deceleration results in an average energy of the protons impinging on the

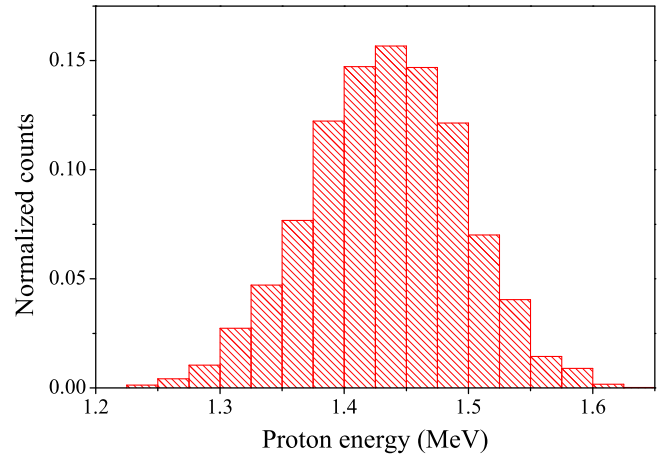


Figure 2. Energy distribution of the protons after crossing the 80 μm thick Al foil (and before impinging on the sample). The counts are normalised to the total number of simulated events.

superconducting film of $1.43 \pm 0.07 \text{ MeV}$. The energy distribution of the protons after crossing the 80 μm thick Al foil (and before impinging on the sample) is reported in figure 2.

Details of the irradiation experiment (e.g. the choice of the Al foil's thickness, the adopted fluences) were guided by previous accurate simulations of the damage induced both in the film and in the substrate, obtained by the Monte Carlo code SRIM [19]. In all cases, protons crossed the films and were implanted into the substrate. The implantation depths in the CaF_2 substrate are 86 μm without Al foil and 21 μm with the 80 μm thick Al foil. The implantation profiles are shown in figure 3. Protons are expected to produce random point defects and some defect nanoclusters in the film/substrate [20], due to the Coulomb scattering with atomic nuclei. SRIM calculations predict a homogeneous energy release along the superconducting film's thickness (100 nm). The Bragg peak is located in the substrate in correspondence to the implantation peak. Following [21], we estimated the expected damage in the film, in terms of displacements per atom (d.p.a.), using the modified Kinchin Pease approach and assuming a displacement energy of 25 eV for all atoms of the target [22]. The average d.p.a. in the $\text{FeSe}_{0.5}\text{Te}_{0.5}$ films are summarised in table 1 for each irradiation experiment together with the lower limit of the average distance between proton-induced defects inferred by d.p.a., disregarding possible Frenkel pairs clustering and annealing effects.

Electrical transport properties of the micro-bridges A and B as a function of temperature and magnetic field were measured in a Physical Properties Measuring System (PPMS) by Quantum Design up to 9 T, while micro-bridges C were characterised in a Cryogenic Free Measurement System (CFMS) by Cryogenic Ltd up to 16 T. Resistivity measurements as a function of the applied magnetic field were performed by the standard four-probe current-biased measurement technique. Critical current values at different temperatures and magnetic fields were extracted from voltage versus current characteristics acquired in the PPMS by sweeping the current from zero with exponentially increasing steps, with the aim to avoid heating problems. CFMS current–voltage measurements

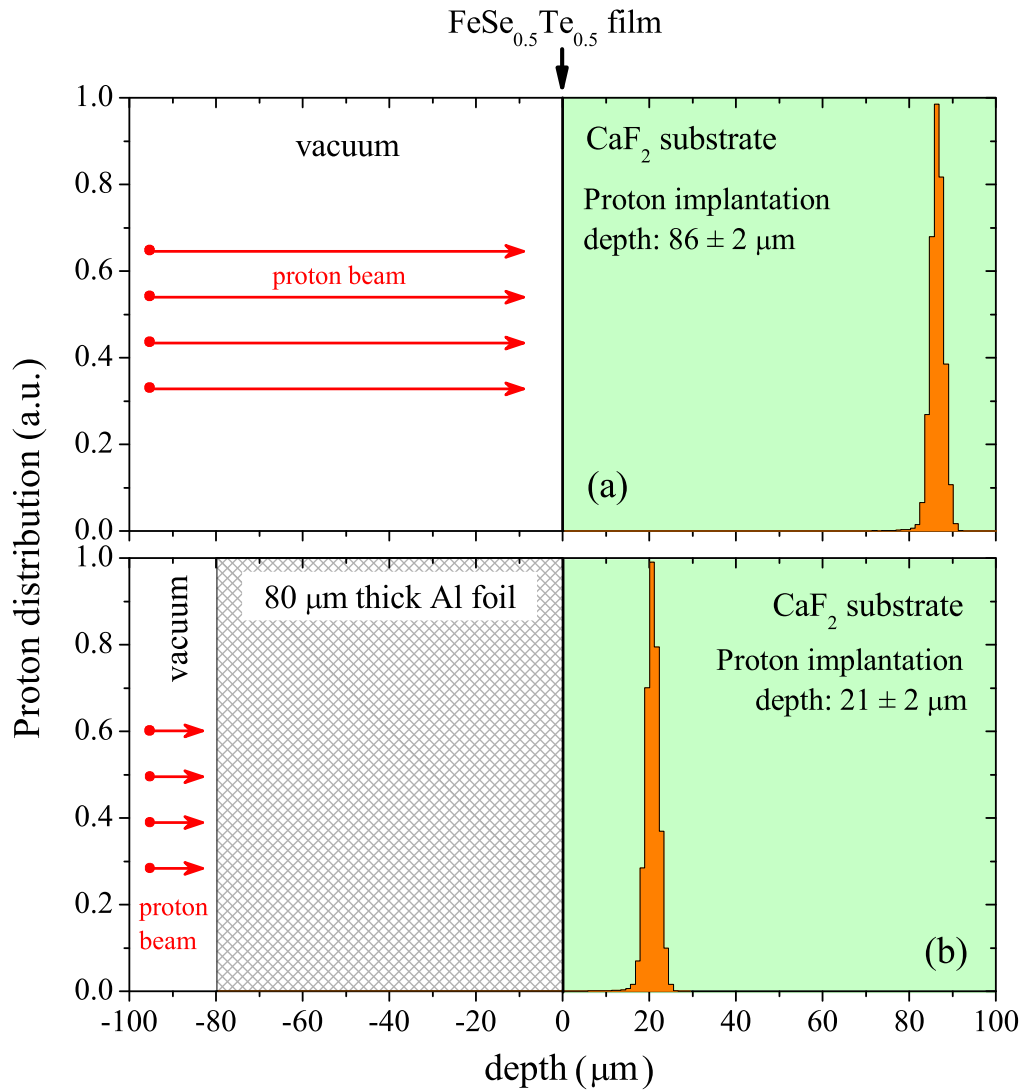


Figure 3. Spatial distribution of the implanted protons (histograms) in the CaF_2 substrate (right regions) (a) without and (b) with the interposition of a $80\ \mu\text{m}$ thick Al foil (crosshatch region) used to decelerate the protons. The zero depth corresponds to the sample surface. The sample consists of a $100\ \text{nm}$ thick $\text{FeSe}_{0.5}\text{Te}_{0.5}$ film (not visible) and its CaF_2 substrate. The interposition of the Al foil results in a shift of the implantation peak closer to the film–substrate interface.

were taken by the delta mode four-probe technique *ad hoc* modified in order to minimise possible heating effects. In this configuration, the current bias is pulsed; each pulse is rectangular in shape with a power-on time of $100\ \text{ms}$ and an inter-pulse spacing of $2\ \text{s}$. The pulse amplitude is increased linearly. The critical current value was defined with the $10\ \mu\text{V cm}^{-1}$ criterion.

Results

Table 1 summarises the irradiation fluences of all the different Hall bars of each sample, and the corresponding calculated d. p.a. values and average distance between defects. Hall bars, irradiated with different fluences, are indicated by a name composed of a letter, which refers to the sample, and a number, which corresponds to the d.p.a. induced by irradiation. It is worth noting that the same fluence can correspond to

different d.p.a. values depending on the energy of protons impinging on the film.

For all samples, there is a pristine reference. For patterned samples there is a pristine Hall bar that is a non-irradiated bar; meanwhile, samples used for x-ray diffraction analysis were also measured before irradiation. It is important to have pristine data as a reference of the properties of the films before irradiation. Indeed, for PLD-deposited films, the sample-to-sample variability of transport properties may be comparable to the effects of irradiation that we are investigating. In the forthcoming figures, we adopt the following legend: symbol shapes identify the sample, and grayscale is a qualitative measure of the irradiation dose (from empty symbols for the unirradiated Hall bars to an increasingly dark colour for increasing dose).

The microstructural parameters describing the lattice strain can be calculated by Rietveld refinement and obtaining the Williamson–Hall plots drawn in figure 4; in particular,

Table 1. Summary of the samples with the relative fluences, average d.p.a, and distance between defects. Samples A, B, and E were directly irradiated with 3.5 MeV protons, while samples C and D were irradiated with protons decelerated through the interposition of a 80 μm thick Al foil. The inter-defect distance was evaluated by considering just stable Frenkel pairs defects, and neglecting possible clustering and annealing effects. Samples D and E used for x-ray diffraction analysis both before and after irradiation were not patterned.

| Sample | Hall bar | Fluence (10^{16} cm^{-2}) | d.p.a | Inter-defect distance (nm) |
|--|----------|---------------------------------------|----------------------|----------------------------|
| A | A_0 | 0 | 0 | — |
| | A_0.25 | 0.70 | $2.5 \cdot 10^{-4}$ | 4.3 |
| | A_0.99 | 2.80 | $9.9 \cdot 10^{-4}$ | 2.7 |
| B | B_0 | 0 | 0 | — |
| | B_0.69 | 1.95 | $6.9 \cdot 10^{-4}$ | 3.1 |
| | B_2.27 | 6.40 | $2.27 \cdot 10^{-3}$ | 2.1 |
| | B_2.59 | 7.30 | $2.59 \cdot 10^{-3}$ | 2.0 |
| C (with 80 μm Al foil) | C_0 | 0 | 0 | — |
| | C_2.30 | 2.68 | $2.30 \cdot 10^{-3}$ | 2.1 |
| | C_4.59 | 5.35 | $4.59 \cdot 10^{-3}$ | 1.6 |
| D_0 | — | 0 | 0 | — |
| D_2.30 (with 80 μm Al foil) | — | 2.68 | $2.30 \cdot 10^{-3}$ | 2.1 |
| D_4.59 (with 80 μm Al foil) | — | 5.35 | $4.59 \cdot 10^{-3}$ | 1.6 |
| E_0 | — | 0 | 0 | — |
| E_1.90 | — | 5.35 | $1.90 \cdot 10^{-3}$ | 2.2 |

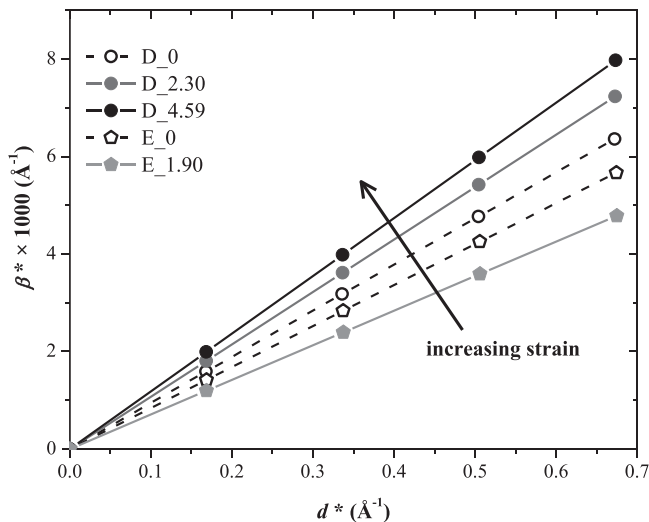


Figure 4. Superposition of Williamson–Hall plots of samples D and E before and after irradiation (β^* : reciprocal integrated breadth of the diffraction line; d^* : reciprocal interplanar spacing).

these plots provide qualitative information about the evolution of the lattice strain along $[001]$ as a function of the irradiation. As expected, the pristine samples D and E are characterised by about the same amount of lattice strain; remarkably, after irradiation they display opposite behaviours. In fact, sample E exhibits a decrease in lattice strain, whereas, conversely, samples pertaining to the D series undergo a progressive increase of the strain with irradiation. This behaviour is clearly related to the different irradiation treatments experienced by these samples. In particular, decelerated protons more effectively produce lattice strain within the thin film; furthermore, the decrease of the strain in sample E could be ascribed to a weak annealing process due to a local heating of the substrate during irradiation. In sample D this effect is likely masked by the higher defect density induced by protons

directly in the film (greater d.p.a. values) and, especially, in the substrate (since protons implant closer to the film–substrate interface), thus increasing the film’s strain.

In figure 5 we show as a reference the critical current density as a function of the magnetic field up to 16 T measured on the pristine sample C_0 at 4.2 K, 8 K, and 12 K. The J_c values for samples A_0 and B_0 are about 20% lower: at 4.2 K and 7 T, J_c is $\approx 2 \cdot 10^5 \text{ A cm}^{-2}$ for sample C_0 and $\approx 1.6 \cdot 10^5 \text{ A cm}^{-2}$ for samples A_0 and B_0. We always compared the irradiated samples with their pristine reference sample, where pristine means a bar measured both before irradiation and after the irradiation process, during which that bar was kept shielded, in order to rule out any spurious or ageing effects.

In figures 6 and 7 we report the J_c values as a function of the field for the patterns irradiated at the different fluences, where J_c has been normalised to the value of pristine sample A_0, B_0, or C_0. The magnetic field was applied perpendicular to the ab crystalline plane, and the temperature was fixed at 4.2 K (figure 6) and 12 K (figure 7). Sample A (squares) and sample B (triangles) were measured up to 9 T, while sample C (circles) was measured up to 16 T. Samples A and B show an improvement of J_c with the increasing dose. In particular, the bar B_2.27 shows an improvement of J_c of about 40% at 7 T and 4.2 K compared to its pristine counterpart. The most irradiated bar of sample B (B_2.59) is not reported at 4.2 K because J_c was too high to be measured for the current supply of the PPMS. At 12 K, as shown in figure 6, the most irradiated bar of sample B (B_2.59) shows an improvement of J_c of about 50% at 7 T. On the contrary, for sample C, an opposite trend is observed, namely, the most irradiated bar C_4.59 shows the worst J_c both in self-field and in-field at all the investigated temperatures. The decrease of J_c at 7 T is about 80% at 4.2 K and almost 90% at 12 K. Hence, from these plots, J_c does not seem to have a monotonic and unique response to irradiation: samples A and B show an

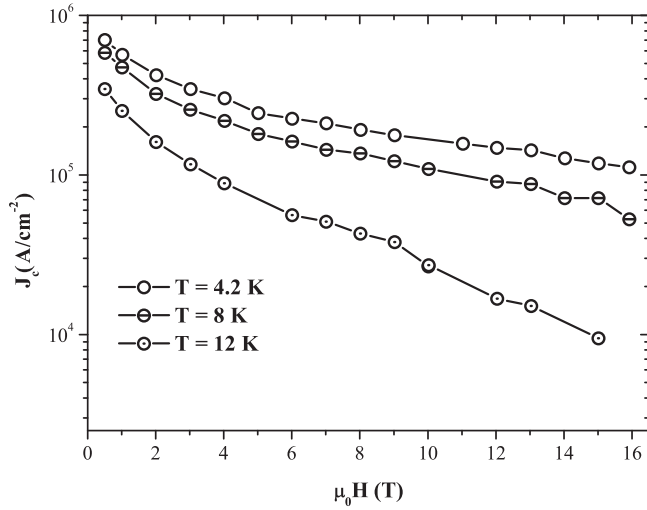


Figure 5. J_c of the pristine sample C versus magnetic field up to 16 T at 4.2 K, 8 K, and 12 K.

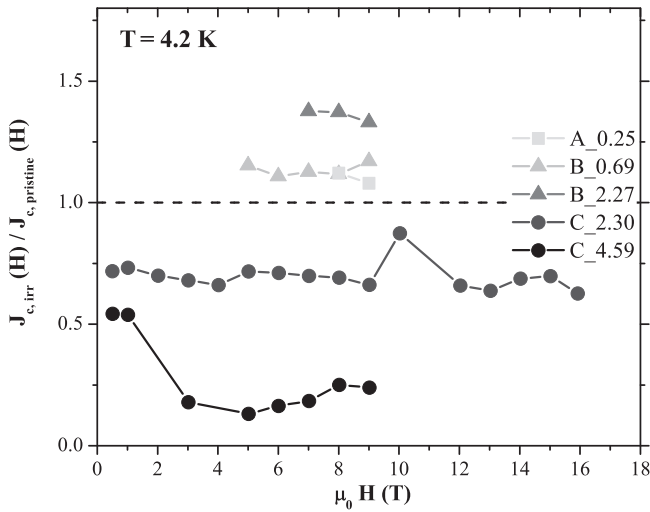


Figure 6. J_c versus magnetic field at 4.2 K for the different irradiated patterns normalised to the values of the relative pristine samples at the same fields.

enhancement of J_c with increasing dose of irradiation, whereas sample C shows the opposite trend. Moreover, we observe that at 4.2 K the in-field behaviour of J_c ratios can be considered flat for all the three samples in the investigated field range, while at 12 K J_c ratios increase with increasing field for samples A and B (where we observe an improvement of J_c with irradiation) and decrease with increasing field in samples C (where J_c decreases upon irradiation).

For a better evaluation of the effects of proton irradiation on J_c , we analysed J_c values at fixed temperatures and fields as a function of the d.p.a. in order to take into account not only the number of particles that hit the target but also the expected damage they induced in the film depending on their energy. Figures 8 and 9 show J_c values, normalised to the value of the corresponding pristine samples A_0, B_0, or C_0, as a function of d.p.a. for all the irradiated bars at 4.2 K and 12 K and at 5 and 9 T. From such plots we observe an increase of J_c

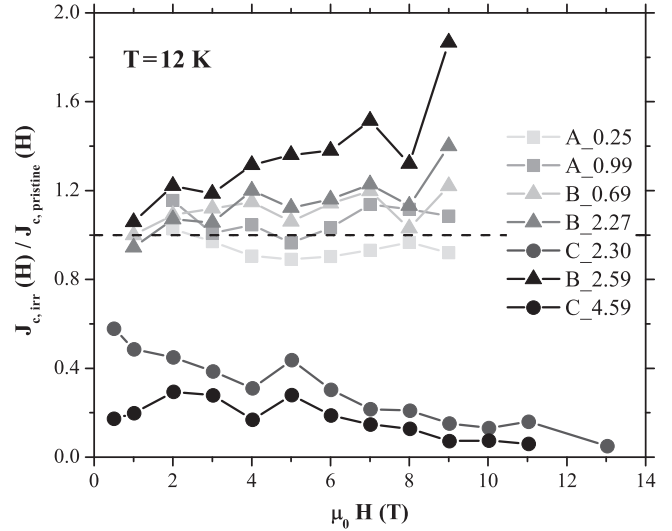


Figure 7. J_c versus magnetic field at 12 K for the different irradiated patterns normalised to the values of the relative pristine samples at the same fields.

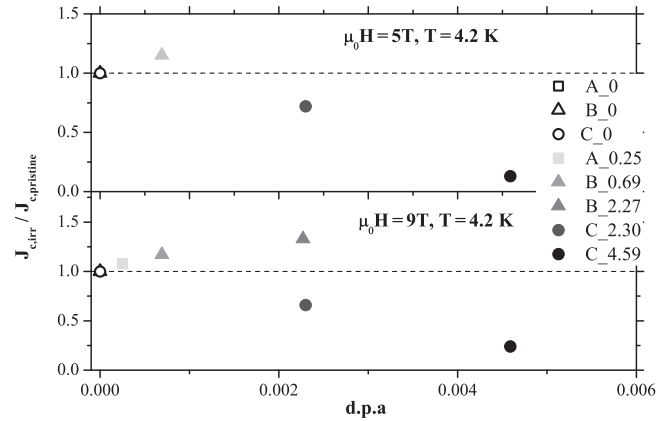


Figure 8. J_c of the irradiated bars normalised to the values of the relative pristine samples at 4.2 K and 5 T (upper panel) and 9 T (lower panel).

for d.p.a. values up to about 0.002 relative to the bars irradiated on sample B: at 9 T J_c increases by 33% at 4.2 K (bar B_2.17) and 86% at 12 K (bar B_2.47). On the contrary, sample C shows a decrease in J_c for a similar d.p.a.. This decrease reaches values of about 75% at 4.2 K and above 90% at 12 K and 9 T, when d.p.a. is over 0.004 (bar C_4.78). This difference in the irradiation effects could be ascribed to the influence of the different defect distribution in the substrate, as discussed in the next section.

In order to evaluate the effect of irradiation on the critical temperature we performed resistivity measurements. In figure 10 we report the resistive transitions for all the bars of the three samples, where the resistivity is normalised to the value of the respective pristine samples at 20 K. We can see that the variations are very small for samples A and B. Only sample A shows a very little decrease of ρ (20 K) of about 5% upon irradiation. Sample C, on the contrary, shows a significant increase in the resistivity of about 20%.

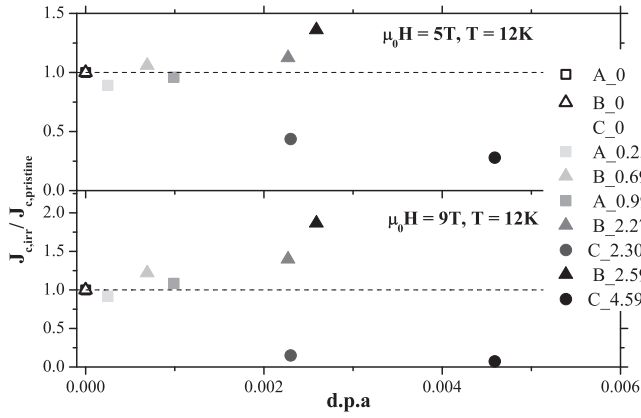


Figure 9. J_c of the irradiated bars normalised to the values of the relative pristine samples at 12 K and 5 T (upper panel) and 9 T (lower panel).

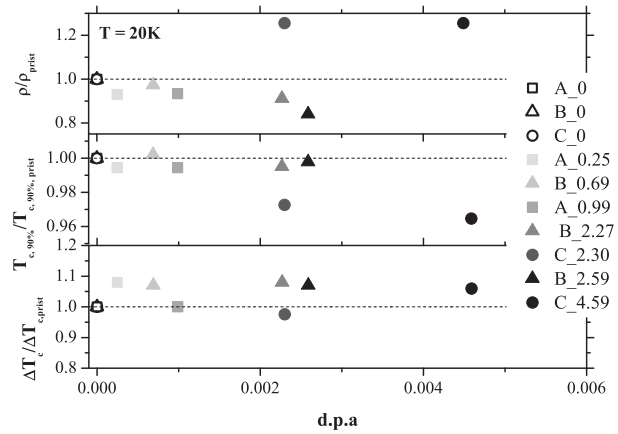


Figure 11. Resistivity at 20 K (top panel), critical temperature (intermediate panel), and ΔT_c (bottom panel) as functions of d.p.a. All quantities have been normalised to the corresponding value of the pristine sample.

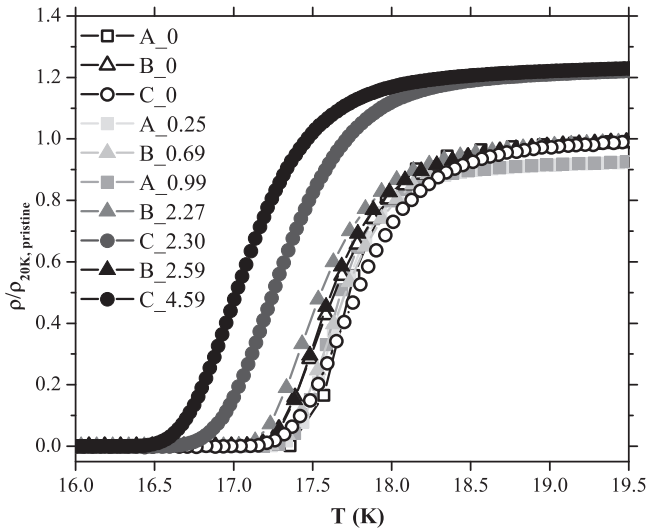


Figure 10. Resistive transitions for all the irradiated bars of samples A, B, and C, where the resistivity at 20 K for each bar is normalised to the resistivity of the relative pristine sample at 20 K.

In figure 11 we report the resistivity in the normal state (20 K), the 90% of the resistive transitions in zero field, and the ΔT_c ($T_{c(90\%)} - T_{c(10\%)}$) for all the irradiated bars, all normalised to the pristine values. As already shown from the resistive transitions, we observe that there is no significant variation of the normal state resistivity in T_c nor in ΔT_c in irradiated samples A and B with respect to the relative pristine sample. In sample C, T_c decreases by about 0.6 K, and, at the same time, the resistivity increases by about 20% upon high-d.p.a. irradiations.

From resistivity measurements in the applied field we evaluated the irreversibility field H_{irr} and upper critical field H_{c2} using the criterion of 10% and 90% of the resistivity value in the normal state above the transition. In figure 12 we report H_{c2} and H_{irr} for all bars, evaluated with $H \parallel c$. In the inset of figure 12, H_{c2} and H_{irr} as a function of the reduced temperature of the corresponding pristine sample are reported. All the curves show very high slopes near T_c , as already

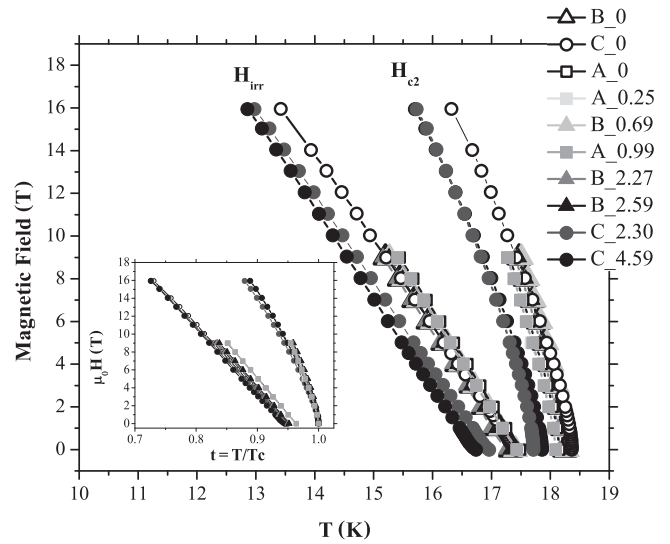


Figure 12. Upper critical field and irreversibility field as a function of temperature for all samples. The inset shows the upper critical field and irreversibility field of all bars as a function of the reduced temperature $t = T/T_c$ of the corresponding pristine sample.

reported for 11 thin films [23, 16]. Irradiation does not significantly change the slope of H_{irr} and H_{c2} curves: indeed, the curves belonging to the same sample are superimposed over each other for samples A and B, while sample C only shows a slight decrease in T_c , as already mentioned above.

Discussion

We have analysed five Fe(Se,Te) thin films deposited on CaF_2 substrates and exposed to proton irradiation at different fluences. For some samples the energy of protons impinging on the film and the implantation depth in the substrate were decreased by the interposition of an Al foil.

As for superconducting properties, the critical fields maintain the same slope as a function of the temperature regardless of different fluences and the presence of the Al foil.

By contrast, the resistivity and critical temperature stay substantially unaltered for samples irradiated without the Al foil, while the slowing down of protons cause a resistivity increase of about 20% and a suppression in T_c of about 0.6 K. For comparison, a T_c suppression of 2 K has been reported in $\text{Ba}(\text{Fe}_{0.925}\text{Co}_{0.075})_2\text{As}_2$ single crystals irradiated with 3 MeV protons and a fluence of $1.2 \cdot 10^{16} \text{ cm}^{-2}$ [24] and up to 4.3 K in $\text{Ba}_x\text{K}_{1-x}\text{Fe}_2\text{As}_2$ single crystals irradiated with 3 MeV protons and a fluence of $9.2 \cdot 10^{16} \text{ cm}^{-2}$ [25].

Regarding the critical current density, samples A and B irradiated directly under the 3.5 MeV proton beam, where the protons implant into the substrate several tens of microns away from the film–substrate interface (see figure 3), were studied for d.p.a. up to 0.0026. In these conditions, we observe an enhancement of J_c upon irradiation. For instance, we measured an improvement of J_c of about 40% at 4.2 K and 7 T, and up to 50% at 12 K, with respect to the pristine bars (see figures 6 and 7). For sample C irradiated with the interposition of an Al foil, which was studied only for d.p.a. higher than 0.002, we found a J_c decrease after irradiation up to 80% at 4.2 K, and of 90% at 12 K and 7 T. We point out that in our experiment, in samples irradiated without Al foil, we did not observe J_c reaching a maximum; meanwhile, in samples irradiated with Al foil, J_c monotonically decreases. Hence, the apparent non-monotonic trend of J_c with increasing d.p.a., i.e. first increase and then decrease, appears only by joining data from differently strained samples; this is also due to the fact that we did not perform experiments in the whole d. p.a. range on a single sample. By comparing these two trends, we can speculate that not only the d.p.a. but also the position of the defects in the substrate can influence the properties of the film, and therefore are able to tune J_c . Indeed, the different behaviour observed in samples A and B with respect to samples C cannot be interpreted in terms of d.p.a. alone. It appears that the interposition of a thin Al foil, which reduces the implantation depth of protons into the substrate, actually modifies the film properties via strain in a different way, depending on whether the substrate is mainly damaged close to or far from the substrate–film interface. In other words, for equal d.p.a., the closer to the interface the irradiation defects in the substrate, the larger the strain in the film and the stronger the detrimental effect on its superconducting properties. This scenario is supported by the x-ray diffraction analysis, from which it appears that the shift of the implantation peak close the interface causes an increase in the strain of the films.

It is worth noting that the J_c enhancement upon irradiation is modest compared to that in other FeSCs families. In [3] it was pointed out that this can be ascribed to the lower depairing current in 11 FeSCs, which sets the magnitude of achievable currents. The moderate J_c enhancement can also be ascribed to the natural presence of pinning centres in Fe(Se, Te) thin films induced by the growth on the CaF_2 substrates [26], where J_c already reaches 10^6 A cm^{-2} (in self-field at 4.2 K), which is about 5% of J_d [3]. The effect of irradiation in the same conditions (3.5 MeV protons) is modest: as a comparison, after irradiation, YBCO thin films show a suppression of J_c of about 20% for d.p.a. as low as $2.04 \cdot 10^{-4}$

[27]. Generally, the low sensitivity of superconducting and normal state properties of this compound to irradiation may result from the balanced competition of positive and detrimental mechanisms. For example, the distribution of irradiation defects may create a coexistence of areas of tensile and compressive stress, having opposite effects on the superconducting properties, and thus resulting in an overall net effect that is small. Only at the largest irradiation doses, and in the presence of a reduced implantation depth into the substrate that can amplify the irradiation-induced effect, the detrimental mechanisms tend to prevail. This robustness of Fe(Se,Te) to irradiation damage is promising for application in magnets for high-energy accelerators.


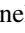
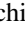
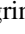
Conclusions

We conducted a study on the effects of irradiation with 3.5 MeV protons on the superconducting properties (critical temperature, fields, and currents) of Fe(Se,Te) thin films grown by PLD on CaF_2 substrates. Fluence was varied in a wide range from 0.7×10^{16} to $7.3 \times 10^{16} \text{ cm}^{-2}$. Moreover, in order to address the issue of the role of the defected substrate where the protons implant in further modifying the film properties, we irradiated some samples with lower proton energies at comparable d.p.a. values by the interposition of a thin Al foil of a suitable thickness. This allows us to control the implantation depth of protons into the substrate, and to check whether the film properties change in a different way when the substrate is mainly damaged close to or far from the substrate–film interface.

It turns out that when protons implant far from the superconducting film, J_c enhancements in $\text{FeSe}_{0.5}\text{Te}_{0.5}$ can be obtained, even if they are not as large as in the case of other FeSCs [3]. In such conditions, critical temperature, and critical and irreversibility fields are virtually unchanged for the employed fluences. Conversely, when the implantation layer is close to the substrate–film interface, both T_c and J_c show a decrease together with an enhancement of resistivity, thus pointing to the crucial role of the substrate itself and its possible modifications in determining superconducting film properties. This should be carefully considered in every irradiation experiment on thin-film superconductors.

Finally, what emerges from our irradiation experiment with MeV-energy protons up to very high values of d.p.a. is that the family Fe(Se,Te) is very robust against proton irradiation with respect to other superconductors, e.g. cuprates. This makes such superconductors very interesting for applications in harsh environments, where strong radiation emissions are expected, such as in accelerators.

ORCID iDs

G Sylva  <https://orcid.org/0000-0001-6301-028X>
 A Martinelli  <https://orcid.org/0000-0001-8391-3486>
 I Pallecchi  <https://orcid.org/0000-0001-6819-6124>
 L Pellegrino  <https://orcid.org/0000-0003-2051-4837>

L Gozzelino  <https://orcid.org/0000-0002-9204-0792>
 D Torsello  <https://orcid.org/0000-0001-9551-1716>
 G Grimaldi  <https://orcid.org/0000-0001-5438-8379>
 V Braccini  <https://orcid.org/0000-0003-0073-367X>

References

- [1] Li J, Guo Y-F, Yang Z-R, Yamaura K, Takayama-Muromachi E, Wang H-B and Wu P-H 2016 *Supercond. Sci. Technol.* **29** 053001
- [2] Ghigo G, Ummarino G A, Gerbaldo R, Gozzelino L, Laviano F, Torsello D and Tamegai T 2017 *Sci. Rep.* **7** 13029
- [3] Eisterer M 2018 *Supercond. Sci. Technol.* **31** 013001
- [4] Fang L *et al* 2013 *Nat. Comm.* **4** 2655
- [5] Eisterer M, Raunicher R, Weber H W, Bellingeri E, Cimberle M R, Pallecchi I, Putti M and Ferdeghini C 2011 *Supercond. Sci. Technol.* **24** 065016
- [6] Mishev V, Eisterer M and Takana Y private communication
- [7] Teknowijoyo S *et al* 2016 *Phys. Rev. B* **94** 064521
- [8] Ozaki T, Wu L, Zhang C, Jaroszynski J, Si W, Zhou J, Zhu Y and Li Q 2016 *Nature Comm.* **7** 13036
- [9] Huang D and Hoffman J E 2017 *Annu. Rev. Condens. Matter Phys.* **8** 311
- [10] Seo S *et al* 2017 *Sci. Rep.* **7** 9994
- [11] Bellingeri E, Pallecchi I, Buzio R, Gerbi A, Marré D, Cimberle M R, Tropeano M, Putti M, Palenzona A and Ferdeghini C 2010 *Appl. Phys. Lett.* **96** 102512
- [12] Tamegai T *et al* 2012 *Supercond. Sci. Technol.* **25** 084008
- [13] Massee F, Sprau P O, Wang Y-L, Séamus Davis J C, Ghigo G, Gu G and Kwok W-K 2015 *Sci. Adv.* **1** e1500033
- [14] Ahmad D, Choi W J, Seo Y I, Seo S, Lee S, Park T, Mosqueira J, Gu G and Kwon Y S 2017 *New J. Phys.* **19** 093004
- [15] Palenzona A *et al* 2012 *Supercond. Sci. Technol.* **25** 115018
- [16] Bellingeri E *et al* 2012 *Supercond. Sci. Technol.* **25** 084022
- [17] Bellingeri E *et al* 2014 *Supercond. Sci. E Technol.* **27** 044007
- [18] Langford J I, Louër D, Sonneveld E J and Visser J W 1986 *Powder Diff.* **1** 211
- [19] Ziegler J F, Ziegler M D and Biersack J P 2010 *Nucl. Instr. Meth. B* **268** 1818
- [20] Haberkorn N, Maiorov B, Usov I O, Weigand M, Hirata W, Miyasaka S, Tajima S, Chikamoto N, Tanabe K and Civale L 2012 *Phys. Rev. B* **85** 014522
- [21] Stoller R E, Toloczko M B, Was G S, Certain A G, Dwaraknath S and Gardner F A 2013 *Nucl. Instrum. Meth. B* **310** 75
- [22] Norgett M J, Robinson M T and Torrens I M 1975 *Nucl. Eng. Des.* **33** 50
- [23] Tarantini C, Gurevich A, Jaroszynski J, Balakirev F, Bellingeri E, Pallecchi I, Ferdeghini C, Shen B, Wen H H and Larbalestier D C 2011 *Phys. Rev. B* **84** 184522
- [24] Nakajima Y, Taen T, Tsuchiya Y, Tamegai T, Kitamura H and Murakami T 2010 *Phys. Rev. B* **82** 220504
- [25] Taen T, Othake F, Akiyama H, Inoue H, Sun Y, Pyon S, Tamegai T and Kitamura H 2013 *Phys. Rev. B* **88** 224514
- [26] Braccini V *et al* 2013 *Appl. Phys. Lett.* **103** 172601
- [27] Gozzelino L, Botta D, Cherubini R, Chiodoni A, Gerbaldo R, Ghigo G, Laviano F, Minetti B and Mezzetti E 2004 *Eur. Phys. J. B* **40** 3